INTERNATIONAL JOURNAL FOR NUMERICAL METHODS IN FLUIDS, VOL. 9, 689–712 (1989)

NUMERICAL STUDY OF THE AXIALLY SYMMETRIC MOTION OF AN INCOMPRESSIBLE VISCOUS FLUID IN AN ANNULUS BETWEEN TWO CONCENTRIC ROTATING SPHERES

JEN-KANG YANG, NICHOLAS J. NIGRO AND ABDEL F. ELKOUH

Department of Mechanical Engineering, Marquette University, Milwaukee, Wisconsin 53233, U.S.A.

AND

JOHN C. GAGLIARDI

Bureau of Mines Research Division, Fort Snelling, Minnesota, U.S.A.

SUMMARY

The research reported herein involved the study of the transient motion of a system consisting of an incompressible Newtonian fluid in an annulus between two concentric, rotating, rigid spheres. The primary purpose of the research was to study the use of a numerical method for analysing the transient motion that results from the interaction between the fluid in the annulus and the spheres which are started suddenly by the action of prescribed torques. The problems considered in this research included cases where: (a) one or both spheres rotate with prescribed constant angular velocities and (b) one sphere rotates due to the action of an applied constant or impulsive torque.

In this research the coupled solid and fluid equations were solved numerically by employing the finite difference technique. With the approach adopted in this research, only the derivatives with respect to spatial variables were approximated with the use of the finite difference formulae. The steady state problem was also solved as a separate problem (for verification purposes), and the results were compared with those obtained from the solution of the transient problem. Newton's algorithm was employed to solve the algebraic equations which resulted from the steady state problem, and the Adams fourth-order predictor–corrector method was employed to solve the ordinary differential equations for the transient problem. Results were obtained for the streamfunction, circumferential function, angular velocity of the spheres and viscous torques acting on the spheres as a function of time for various values of the system dimensionless parameters.

KEY WORDS Rotating spheres Viscous flow Incompressible fluid

INTRODUCTION

The problem involving the steady state motion of a viscous incompressible fluid contained in an annulus between two concentric spheres which rotate about a common axis with an angular velocity which has been prescribed *a priori* has been the subject of extensive research in engineering, meteorology and geophysics. Proudman,[1] Stewartson,[2] Carrier,[3] Haberman[4] and Munson and Joseph[5] obtained an approximate analytical solution to the problem involving the flow in an annulus between two spheres rotating with prescribed constant angular velocities. Pedlosky[6] extended the problem to include temperature effects. Dennis and Singh[7] solved this

0271–2091/89/060689–24$12.00

Received 20 October 1987
Revised 16 June 1988

problem by employing a quasi-analytical method; i.e. they expanded the streamfunction, vorticity and circumferential function in a series of orthogonal functions and then solved the resulting system of ordinary differential equations numerically. Greenspan,[8] Schultz and Greenspan,[9] Schrauf[10] and Bar-Yoseph *et al.*[11] solved this problem by employing the numerical finite difference and finite element methods.

Experimental results have been obtained for the steady state problem by a number of investigators. Sorokin *et al.*,[12] Khlebutin,[13] Zierep and Sawatzki,[14] Munson and Menguturk,[15] Wimmer,[16,17] Nakabayashi[18] and Waked and Munson[19,20] studied the problem involving flow in an annulus between two spheres where either the inner or the outer sphere rotates with constant angular velocity. Munson and Douglas[21] obtained experimental results for the problem where the inner sphere is subjected to a prescribed oscillatory (sinusoidal) motion.

The problem involving the transient motion of a fluid contained in an annulus between two concentric rotating spheres has received less attention in the literature. Pearson,[22,23] Dennis and Quartapelle,[24] Krause and Bartels[25] and Bartels[26] employed the finite difference method to obtain a solution to the transient problem for the case where one of the spheres is suddenly rotated with a prescribed constant angular velocity. The study of this problem for a sphere rotating in an infinite medium has been conducted by Illingworth,[27] Benton,[28] Barrett,[29] Dennis and Ingham,[30] Dennis *et al.*[31] and Takagi.[32] To date, there has been no published research involving the transient motion of a viscous fluid contained in an annulus between rotating spheres where the angular velocities of the spheres is not prescribed *a priori*; i.e. where the motion of the system is a result of the coupling (interaction) between the fluid and the spheres. Recently, Gagliardi[33] studied this problem for low Reynolds numbers by employing the perturbation technique.

The primary purpose of this research was to study the use of a numerical method for analyzing the transient flow of a viscous incompressible fluid contained in an annulus between two spheres which are started suddenly by the action of prescribed torques instead of prescribed angular velocities. The equations of motion for the rigid body and the fluid were expressed in terms of a streamfunction (Ψ), a circumferential function (Ω) and a vorticity function (ζ) and then reduced to a system of ordinary differential equations by employing the finite difference method. The Adams fourth-order predictor–corrector method was employed to solve these equations. The steady state problem was also solved as a separate problem (for verification purposes) by employing Newton's algorithm. Results for Ψ, Ω, angular velocities of the spheres, viscous torques and fluid angular momentum were obtained as a function of various values of the dimensionless parameters.

BASIC EQUATIONS

The system under study consists of an isothermal, incompressible, Newtonian fluid contained in an annulus between two concentric rotating rigid spheres (see Figure 1). The inner and outer radii of the annulus are R_1^* and R_2^* respectively. The spheres are assumed to be rigid and constrained to rotate about the z^*-axis under the action of externally applied torques.

The fluid velocity components in the direction of the spherical co-ordinates r^*, θ and ϕ are given as u^*, v^* and w^* respectively. These components are independent of the co-ordinate ϕ due to symmetry about the spin axis. The transformation equations which relate the fluid velocity components to the streamfunction (Ψ^*) and circumferential function (Ω^*) are given as

$$u^* = \frac{1}{r^{*2}\sin\theta}\Psi^*_{,\theta}, \qquad v^* = -\frac{1}{r^*\sin\theta}\Psi^*_{,r^*}, \qquad w^* = \frac{\Omega^*}{r^*\sin\theta}, \tag{1}$$

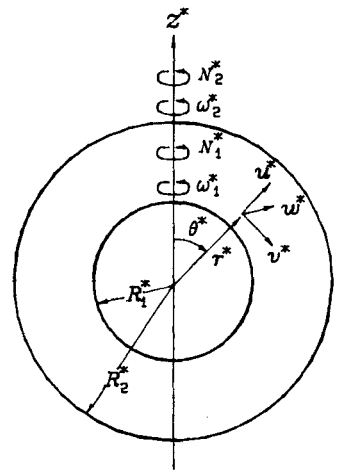

Figure 1. Notation for flow in spherical annulus

where

$$\Psi^*_{,\theta} = \partial\Psi^*/\partial\theta, \qquad \Psi^*_{,r^*} = \partial\Psi^*/\partial r^*.$$

The form of equation (1) for u^* and v^* is such that the continuity equation is automatically satisfied. The system variables in this equation are expressed in dimensionless form by employing the transformations

$$r = r^*/R_0^*, \qquad t = \frac{t^* v^*}{R_0^{*2}}, \qquad \omega = \omega^*/\omega_0^*, \qquad \Psi = \Psi^*/\omega_0^* R_0^{*3}, \qquad \Omega = \Omega^*/\omega_0^* R_0^{*2}, \quad (2)$$

where v^* is the kinematic viscosity, R_0^* is an arbitrary reference radius and ω_0^* is a reference angular velocity.

The equations of motion for the fluid are obtained by taking the curl of the Navier–Stokes equations. This yields

$$\Omega_{,t} - Re_q \frac{\Psi_{,r}\Omega_{,\theta} - \Psi_{,\theta}\Omega_{,r}}{r^2 \sin\theta} = D^2\Omega, \tag{3a}$$

$$\zeta_{,t} + \frac{2Re_q\Omega}{r^2\sin^2\theta}[\Omega_{,r} r\cos\theta - \Omega_{,\theta}\sin\theta] - \frac{Re_q}{r^2\sin\theta}[\Psi_{,r}\zeta_{,\theta} - \Psi_{,\theta}\zeta_{,r}]$$
$$+ \frac{2Re_q\zeta}{r^3\sin^2\theta}[\Psi_{,r} r\cos\theta - \Psi_{,\theta}\sin\theta] = D^2\zeta. \tag{3b}$$

$$\zeta = D^2\Psi, \tag{3c}$$

where

$$\zeta = \zeta^*/\omega_0^* R_0^* \quad (\zeta^* \text{ is the vorticity function}),$$

$$Re_q = \omega_0^* R_q^{*2}/v^* \quad (\text{Reynolds number based on } R_0^* = R_q^*, q = 1, 2), \tag{3d}$$

$$\zeta_{,t} = \frac{\partial\zeta}{\partial t}, \qquad \Omega_{,t} = \frac{\partial\Omega}{\partial t}, \qquad D^2 = \frac{\partial^2}{\partial r^2} + \frac{1}{r^2}\frac{\partial^2}{\partial\theta^2} - \frac{\cot\theta}{r^2}\frac{\partial}{\partial\theta}. \tag{3e}$$

The steady state equations of motion for the fluid are obtained from equation (3) by dropping the transient terms.

The equations of motion for the inner and outer spheres rotating under the action of applied torques are

$$\omega_{q,t} + J_q \int_0^{\pi/2} [R_q(R_q \Omega_{,r}[R_q, \theta, t] - 2\Omega[R_q, \theta, t])] \sin\theta \, d\theta = N_q, \tag{4a}$$

where

$$J_q = (-1)^q 4\pi \rho_f^* R_0^{*5} / I_q^*, \tag{4b}$$

with ρ_f^* the density of fluid and I_q^* the mass moment of inertia of the inner or outer sphere;

$$N_q = N_q^* Re_q / I_q^* \omega_0^{*2}, \tag{4c}$$

with N_q^* the external torque applied to the inner or outer sphere;

$$R_q = R_q^*/R_0^*, \qquad \omega_q = \omega_q^*/\omega_0^*, \tag{4d}$$

with ω_q^* the angular velocity of the inner or outer sphere and $q = 1, 2$ for inner and outer spheres respectively.

The equations which result from the symmetry of the flow in the annulus are

$$\Omega[r, 0, t] = 0, \tag{5a}$$

$$\Omega_{,\theta}[r, \pi/2, t] = 0, \tag{5b}$$

$$\Psi[r, 0, t] = 0, \tag{5c}$$

$$\Psi[r, \pi/2, t] = 0, \tag{5d}$$

$$\zeta[r, 0, t] = 0, \tag{5e}$$

$$\zeta[r, \pi/2, t] = 0, \tag{5f}$$

$$\zeta[R_q, \theta, t] = \Psi_{,rr}[R_q, \theta, t] \quad q = 1, 2. \tag{5g}$$

The conditions which must be satisfied at the interfaces of the fluid and solid are

$$\Psi[R_q, \theta, t] = 0, \tag{6a}$$

$$\Psi_{,r}[R_q, \theta, t] = 0, \tag{6b}$$

$$\Omega[R_q, \theta, t] = \omega_q R_q \sin^2\theta, \quad q = 1, 2. \tag{6c}$$

The fluid inside the spherical annulus is assumed to be initially at rest; hence the initial conditions for the fluid are

$$\Omega[r, \theta, 0] = \Psi[r, \theta, 0] = 0. \tag{7}$$

The cases which are considered in this research consist of the following, or combinations of the following: (a) the inner (or outer) sphere is started suddenly from rest with a prescribed constant angular velocity (i.e. step function input), with the opposite outer (or inner) sphere either fixed or given a different prescribed angular velocity; (b) the inner (or outer) sphere is started from rest by the action of a prescribed impulsive torque, with the opposite outer (or inner) sphere fixed or left free to rotate. The reference angular velocity in case (a) was chosen to be the larger of the two prescribed angular velocities. Note that for this case, equation (4a) is not required since ω_q^* is prescribed. The reference angular velocities for cases involving the prescribed impulsive torque

are given as

$$\omega_0^* = \hat{N}_q^*/I_q^*, \tag{8}$$

where $\hat{N}_q^*$ is the magnitude of the torque impulse.

The viscous torque (T_q^*) acting on the inner or outer sphere can be evaluated by integrating the shearing stress ($\tau_{\phi r}^*$) over the corresponding spherical surface. The expression for the dimensionless torque is given as

$$T_q = \tfrac{3}{2}\int_0^{\pi/2} [R_q(R_q\Omega_{,r}[R_q, \theta, t] - 2\Omega[R_q, \theta, t])] \sin\theta \, d\theta, \tag{9}$$

where:

$$T_q = \left(\frac{3}{8\pi}\right)\frac{T_q^*}{\mu^*\omega_0^* R_0^{*3}}, \qquad \mu^* = \frac{\nu^*}{\rho_f^*}$$

and $q = 1, 2$ for the inner and outer spheres respectively.

The fluid angular momentum (L_f) about the spin axis was employed in this research as a quantitative measure of flow. The expression for the dimensionless angular momentum (L_f) is

$$L_f = 4\pi \int_0^{\pi/2}\int_{R_1}^{R_2} \Omega r^2 \sin\theta \, dr \, d\theta, \tag{10}$$

where

$$L_f = L_f^*/\rho_f^*\omega_0^* R_0^{*5}.$$

METHOD OF ANALYSIS

Finite difference model

In this study, the finite difference method was employed to solve the mathematical model given in equations (3)–(4). For this purpose, the domain was discretized by a uniform mesh as shown in Figure 2. The discretized independent variables r_i and θ_j are defined as

$$r_i = (i-1)\Delta r + r_{12}, \quad i = 1, 2, \ldots, N+1, \tag{11a}$$

$$\theta_j = (j-1)\Delta\theta, \quad j = 1, 2 \ldots, L+1, \tag{11b}$$

where

$$\Delta r = \frac{1-r_{12}}{N}, \qquad r_{12} = \frac{R_1}{R_2}, \qquad \Delta\theta = \frac{\pi}{2L}. \tag{11c}$$

The spatial derivatives of Ω, Ψ and ζ at all boundary and first line interior nodes (see Figure 2) were approximated by employing the fourth-order forward and backward finite difference formulae. The spatial partial derivatives at all other interior nodes were approximated by employing the fourth-order central difference formulae. The transient finite difference model for the fluid was obtained by employing these equations to approximate all those terms in equations (3) involving derivatives with respect to spatial variables. This yields a system of equations of the form

$$\Omega_{i,t}^{(i,j)} = f_1(\Omega, \Psi), \tag{12a}$$

$$\zeta_{i,t}^{(i,j)} = g_1(\Omega, \Psi, \zeta), \tag{12b}$$

$$\zeta = \mathbf{A}\Psi, \tag{12c}$$

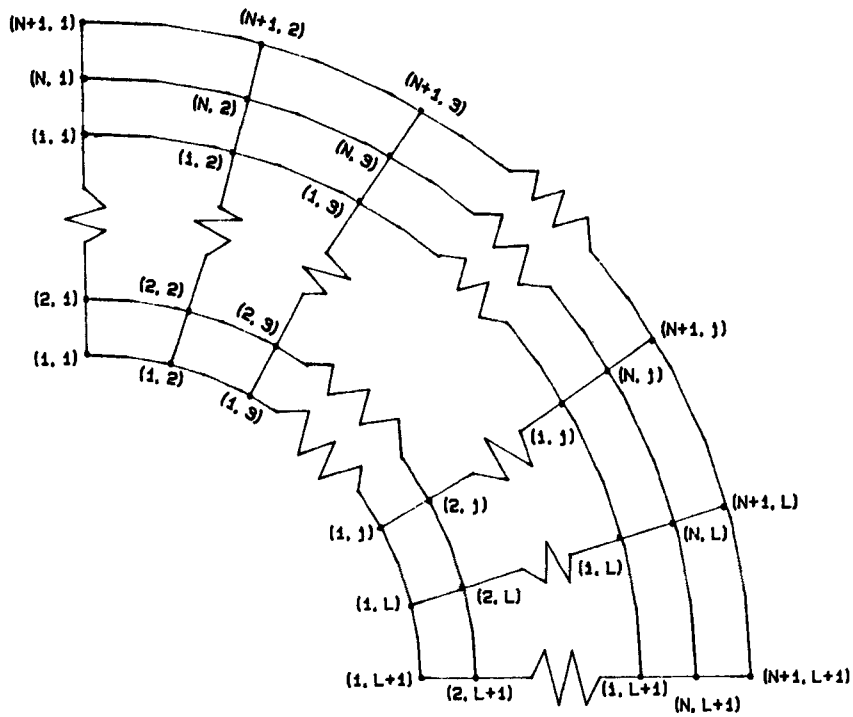

Figure 2. Discretization of region for finite difference method

where

$$\boldsymbol{\Omega}=\begin{bmatrix}\Omega^{(2,2)}\\ \vdots \\ \Omega^{(N,L)}\end{bmatrix}, \qquad \boldsymbol{\Psi}=\begin{bmatrix}\Psi^{(2,2)}\\ \vdots \\ \Psi^{(N,L)}\end{bmatrix}, \qquad \boldsymbol{\zeta}=\begin{bmatrix}\zeta^{(2,2)}\\ \vdots \\ \zeta^{(N,L)}\end{bmatrix},$$

$$\Omega_{l,t}=\mathrm{d}\Omega_l/\mathrm{d}t, \qquad \zeta_{l,t}=\mathrm{d}\zeta/\mathrm{d}t, \qquad \mathbf{A}=[a_{ij}],$$

f_l, g_l, a_{ij} are functions defined in Reference 34, and

$$i=2,\ldots,N, \qquad j=2,\ldots,L, \qquad l=1,\ldots,(N-1)\,(L-1).$$

The variable ζ was eliminated from equations (12) by differentiating equation (12c) with respect to time, inverting the resulting equation for $\boldsymbol{\Psi}_{,t}$ and employing this in conjunction with equations (12b) and (12c). This yields

$$\Omega_{l,t}^{(i,j)}=f_l(\boldsymbol{\Omega},\boldsymbol{\Psi}), \tag{13a}$$

$$\Psi_{l,t}^{(i,j)}=h_l(\boldsymbol{\Omega},\boldsymbol{\Psi}) \tag{13b}$$

where h_l are functions defined in Reference 34.

The finite difference form of the boundary equations was obtained by employing the forward and backward finite difference formulae. This yields

$$\Omega^{(i,1)}=0, \quad i=2,\ldots,N, \tag{14a}$$

$$\Omega^{(i,L+1)}=\tfrac{1}{25}[48\Omega^{(i,L)}-36\Omega^{(i,L-1)}+16\Omega^{(i,L-2)}-3\Omega^{(i,L-3)}], \quad i=2,\ldots,N, \tag{14b}$$

$$\Psi^{(i,1)}=0, \quad i=2,\ldots,N, \tag{14c}$$

$$\Psi^{(i,L+1)}=0, \quad i=2,\ldots,N, \tag{14d}$$

$$\zeta^{(i,1)}=0, \quad i=1,\ldots,N+1, \tag{14e}$$

$$\zeta^{(i,L+1)}=0, \quad i=1,\ldots,N+1, \tag{14f}$$

$$\zeta^{(1,j)}=\frac{16\Psi^{(2,j)}-\Psi^{(3,j)}}{6\Delta r^2}, \quad j=2,\ldots,L, \tag{14g}$$

$$\zeta^{(N+1,j)}=\frac{16\Psi^{(N,j)}-\Psi^{(N-1,j)}}{6\Delta r^2}, \quad j=2,\ldots,L, \tag{14h}$$

$$\Psi^{(1,j)}=0, \quad j=1,\ldots.L+1, \tag{14i}$$

$$\Psi^{(N+1,j)}=0, \quad j=1,\ldots,L+1, \tag{14j}$$

$$\Omega^{(1,j)}=\omega_1 R_1^2 \sin^2\theta_j, \quad j=1,\ldots,L+1, \tag{14k}$$

$$\Omega^{(N+1,j)}=\omega_2 R_2^2 \sin^2\theta_j, \quad j=1,\ldots,L+1. \tag{14l}$$

The final form of the finite difference model (including the boundary equations) for the transient case was obtained by combining equations (13) and (14). The general form of this model can then be written as

$$\mathbf{q}_{k,t}=\mathbf{G}_k, \tag{15}$$

Table I. Case study designations: (a) prescribed angular velocity problem; (b) impulsive torque problem

(a)	Case I $R_1/R_2=0{\cdot}90$		Case II $R_1/R_2=0{\cdot}50$				Case III $\dot{R}_1/R_2=0{\cdot}20$	
	A	B	A	B	C	D	A	B
	$\omega_1=1$	$\omega_1=0$	$\omega_1=1$	$\omega_1=0$	$\omega_1=-1$	$\omega_1=1$	$\omega_1=1$	$\omega_1=0$
Re_2	$\omega_2=0$	$\omega_2=1$	$\omega_2=0$	$\omega_2=1$	$\omega_2=1$	$\omega_2=-0{\cdot}5$	$\omega_2=0$	$\omega_2=1$
100	a-IA-1	a-IB-1	a-IIA-1	a-IIB-1	a-IIC-1	a-IID-1	a-IIIA-1	a-IIIB-1
500	a-IA-2	a-IB-2	a-IIA-2	a-IIB-2	a-IIC-2	a-IID-2	a-IIIA-2	a-IIIB-2
1000	a-IA-3	a-IB-3	a-IIA-3	a-IIB-3	a-IIC-3	a-IID-3	a-IIIA-3	a-IIIB-3
2000	a-IA-4	a-IB-4	a-IIA-4	a-IIB-4	a-IIC-4	a-IID-4	a-IIIA-4	a-IIIB-4
3000	a-IA-5	a-IB-5	a-IIA-5	a-IIB-5	a-IIC-5	a-IID-5	a-IIIA-5	a-IIIB-5

(b)	Case I $R_1/R_2=0{\cdot}90$ $-J_1=J_2=1{\cdot}63588$		Case I $R_1/R_2=0{\cdot}90$ $-J_1=J_2=4{\cdot}58045$		Case II $R_1/R_2=0{\cdot}50$ $-J_1=J_2=3{\cdot}09110\text{E}1$		Case III $R_1/R_2=0{\cdot}20$ $-J_1=J_2=3{\cdot}01865\text{E}3$	
	A	B	C	D	A	B	A	B
	$\omega_1(0)=1$	$\omega_1=0$	$\omega_1(0)=1$	$N_1=0$	$\omega_1(0)=1$	$\omega_1=0$	$\omega_1(0)=1$	$\omega_1=0$
Re_2	$\omega_2=0$	$\omega_2(0)=1$	$N_2=0$	$\omega_2(0)=1$	$\omega_2=0$	$\omega_2(0)=1$	$\omega_2=0$	$\omega_2(0)=1$
100	b-IA-1	b-IB-1	b-IC-1	b-ID-1	b-IIA-1	b-IIB-1	b-IIIA-1	b-IIIB-1
1000	b-IA-2	b-IB-2	b-IC-2	b-ID-2	b-IIA-2	b-IIB-2	b-IIIA-2	b-IIIB-2

where

$$\mathbf{q}=[\Omega, \Psi, \omega_1, \omega_2]^T, \quad \mathbf{G}=\mathbf{G}(\Omega, \Psi, \omega_1, \omega_2, t), \quad k=1, \ldots, 2(N-1)\times(L-1)+2.$$

The general form of the finite difference model for the steady state problem was obtained by dropping the transient terms in equation (15). This yields

$$\mathbf{G}_k(\Omega, \Psi, \omega_1, \omega_2)=0, \tag{16}$$

$$k=1, 2, \ldots, 2(N-1)\times(L-1)+2.$$

Numerical solution of finite difference models

The finite difference equations for the steady state problem (equation (16)) were solved iteratively by employing Newton's algorithm. The equations for the transient problem (equation (15)) were solved by employing the explicit Adams fourth-order predictor–corrector method. This method is based on employing the third-order Adams–Bashforth algorithm for the predictor formula and the fourth-order Adams–Moulton algorithm for the corrector formula. The necessary starting values were obtained by employing the fourth-order Runge–Kutta algorithm. The viscous torque (equation (9)) and the angular momentum of the fluid (equation (10)) were evaluated by employing Simpson's rule.

RESULTS

A computer program was developed to evaluate Ω, Ψ, T_q and L_f for each of the case study problems. Numerical results were obtained by running this program in double precision for various values of the dimensionless parameters. The designations for the different case studies which are discussed in this paper are given in Tables I(a) and I(b). Results for other case studies, including the constant torque problem, are discussed in Reference 34. Future reference to the results obtained from a particular case study will be made by employing the unit code in the tables; e.g. a-IA-1 refers to the prescribed angular velocity problem (a) with $R_1/R_2=0{\cdot}9$, $\omega_1=1$, $\omega_2=0$ and $Re_2=100$.

Mesh size

The mesh size required to obtain the desired precision for a specific Reynolds number (Re_q) was based on the prescribed angular velocity problem, such that at steady state: (a) the values obtained for the dimensionless torques at the inner and outer spheres were equal and opposite; and (b) the dimensionless angular momentum for the fluid in the annulus attained a limiting value. Results were obtained with decreasing mesh size until both of these conditions were satisfied within three significant figures. Tyical results illustrating the effect of mesh size are shown in Table II. In general it was found that the required mesh size decreased with increasing Reynolds number and radius ratio R_2/R_1.

Results for prescribed angular velocity problem

Numerical results for Ω and Ψ were obtained as a function of r, θ and t for all of the case studies designated in Table I(a). Typical results for the Ω and Ψ contours are shown in Figures 3–11. Contour plots for additional case studies can be found in Reference 34. As can be seen, for $Re_2=100$ the contours shown in Figures 3–6 are in close agreement with those obtained by Gagliardi.[33] Although not shown here, the contours presented in Figures 7–8 are also in good agreement with those obtained by other investigators.[5,7,11,22] However, the contours in Figures

Table II. Effect of mesh size for case a-IIA-2

Mesh size($r \times \theta$)	$-T_1$	T_2	L_f
8×8	0·86469	0·56228	0·18839
10×10	0·82679	0·62159	0·19281
12×12	0·79996	0·67159	0·19706
10×20	0·82614	0·70274	0·20537
16×16	0·76955	0·74106	0·20397
16×20	0·76918	0·76669	0·20744
16×24	0·76909	0·77084	0·20811
16×26	0·76909	0·76850	0·20711

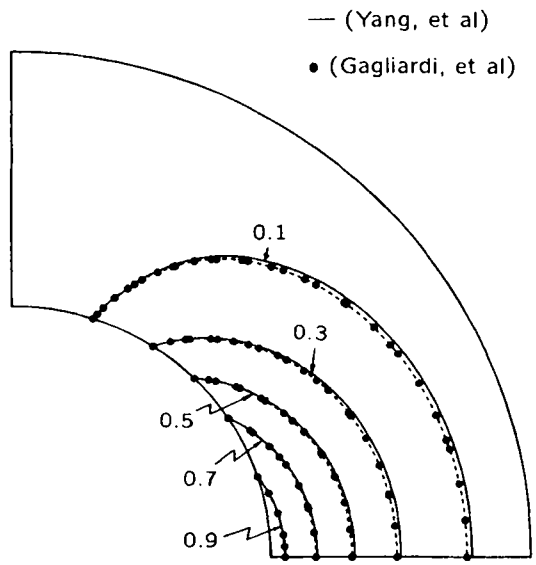

Figure 3. Plot of contour lines for Ω; case study a-IIA-1 ($t = 0{\cdot}03$)

9 and 10 ($Re_2 = 3000$) are in slight disagreement with those obtained by Schultz and Greenspan.[9] This is probably due to the fact that they employed lower-order finite difference derivative formulae. Figure 11 illustrates the transient motion in the meridional plane at an early stage. A comparison of Figure 11 with Figure 7 indicates the development of the fluid motion.

Values for the viscous torques (T_q) for several cases are presented as a function of time in Figures 12–14. These figures show that the magnitudes of the viscous torques T_1 and T_2 attain the same asymptotic value at steady state. In general, although not shown in the figures, the time required to attain steady state increases with decreasing radius ratio R_1/R_2. Figure 12 also shows that the values for T_q obtained from this investigation are in good agreement with those obtained by Gagliardi.[33]

The results for the steady state viscous torques (T_q) are plotted as a function of the radius ratio R_2/R_1 for $Re_1 = 15$ and 45 in Figures 15 and 16. The results in these figures are shown compared to: (a) the limiting values ($R_2/R_1 \to \infty$) obtained from Dennis *et al.*;[31] (b) values predicted by the Couette flow theory ($R_2/R_1 \to 1$); and (c) values obtained by Gagliardi.[33] The values in the figures

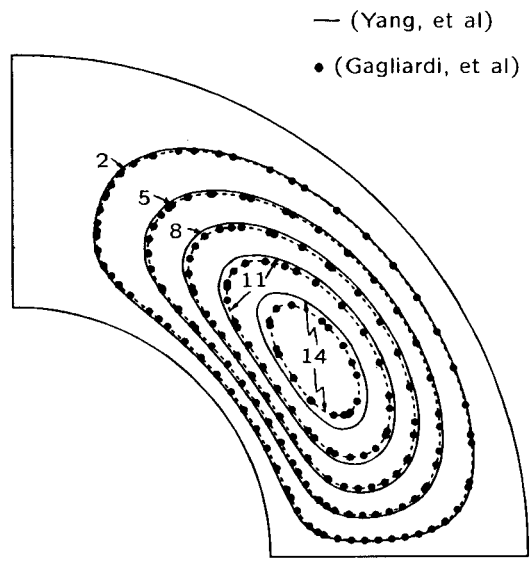

Figure 4. Plot of contour lines for $-\Psi \times 10^4$; case study a-IIA-1 ($t=0{\cdot}03$)

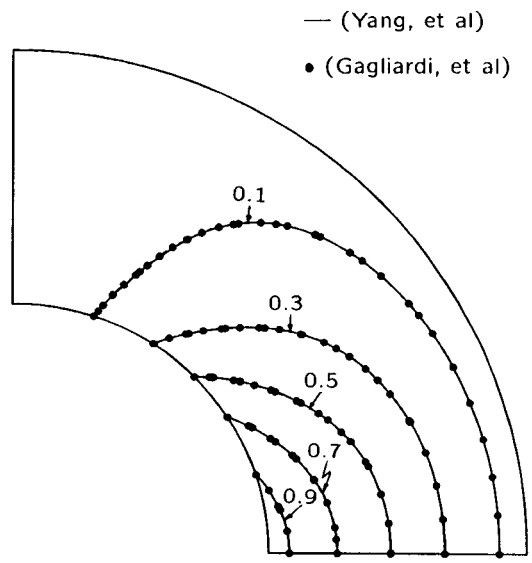

Figure 5. Plot of contour lines for Ω; case study a-IIA-1 (steady state)

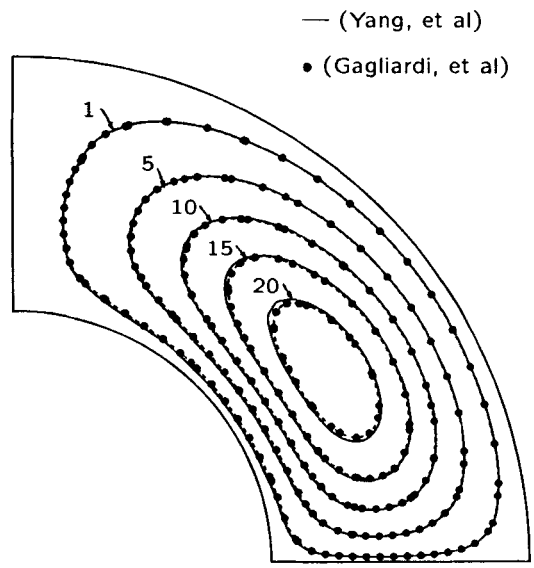

Figure 6. Plot of contour lines for $-\Psi \times 10^4$; case study a-IIA-1 (steady state)

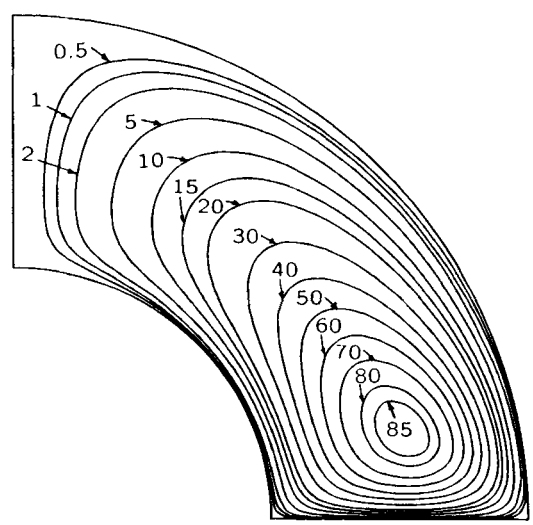

Figure 7. Plot of contour lines for $-\Psi \times 10^4$; case study a-IIA-3 (steady state)

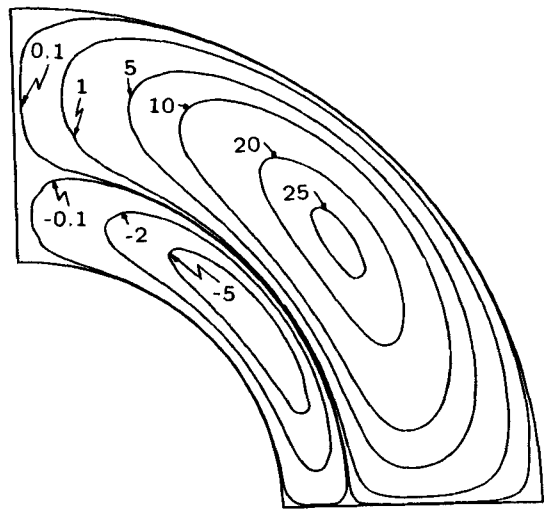

Figure 8. Plot of contour lines for $\Psi \times 10^4$; case study a-IID-2 (steady state)

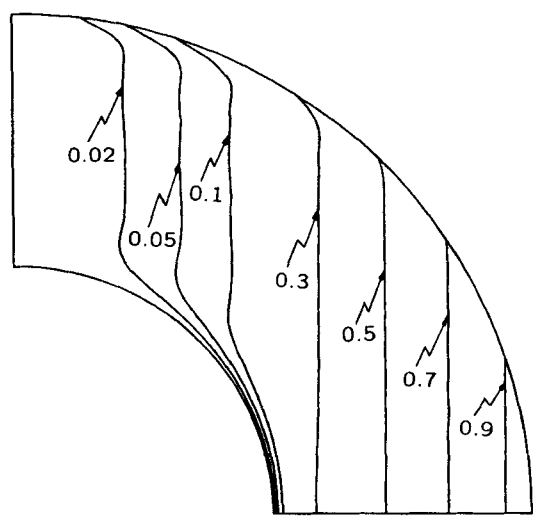

Figure 9. Plot of contour lines for Ω; case study a-IIB-5 (steady state)

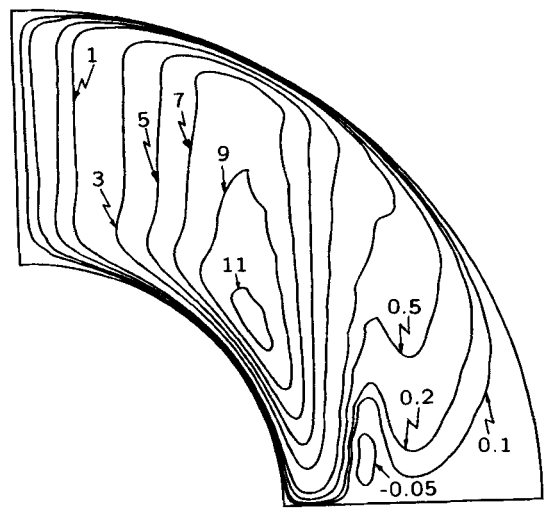

Figure 10. Plot of contour lines for $\Psi \times 10^4$; case study a-IIB-5 (steady state)

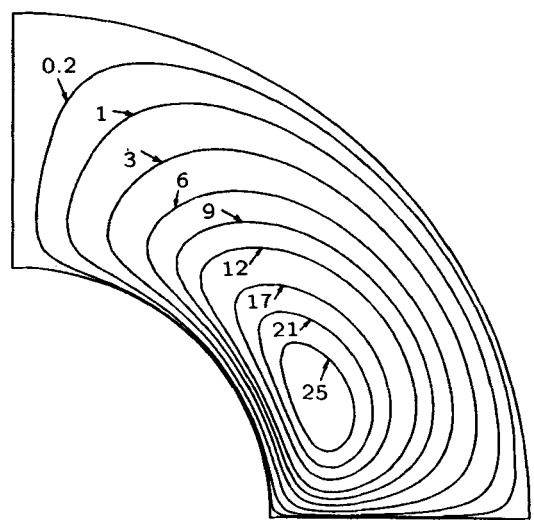

Figure 11. Plot of contour lines for $-\Psi \times 10^4$; case study a-IIA-3 ($t = 0{\cdot}005$)

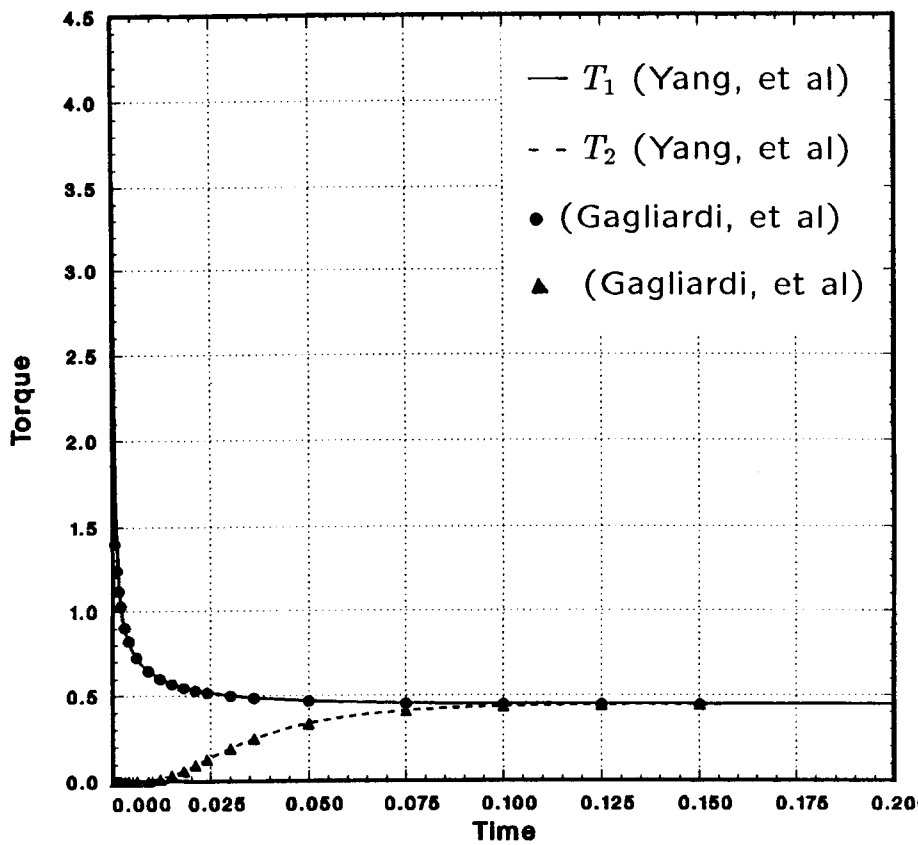

Figure 12. Plot of viscous torque versus time; case study a-IIA-1

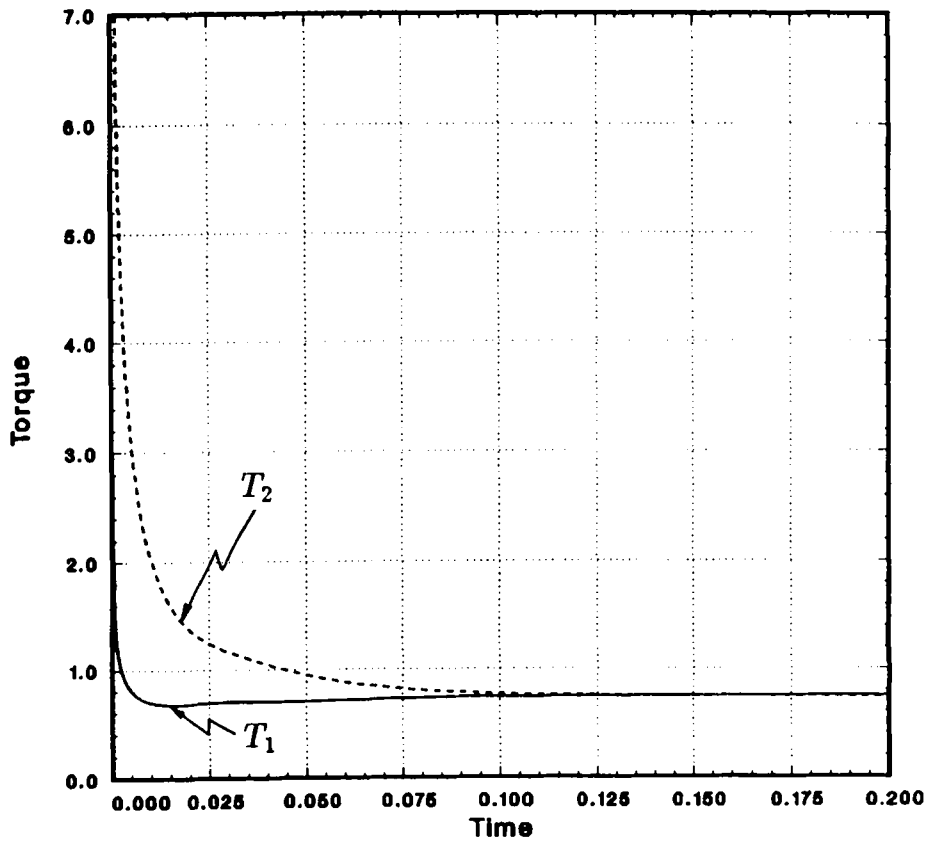

Figure 13. Plot of viscous torque versus time; case study a-IID-2

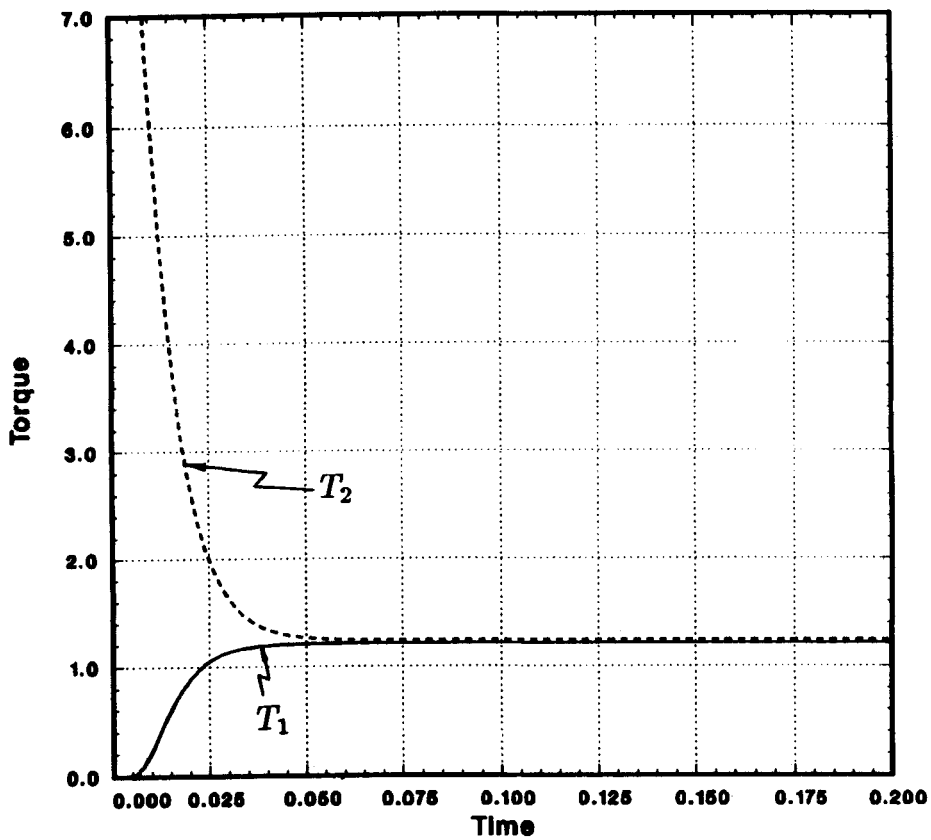

Figure 14. Plot of viscous torque versus time; case study a-IIB-5

are in good agreement with those obtained by Dennis *et al.*[31] for $R_2/R_1 \to \infty$. These figures indicate that an annulus with $R_2/R_1 \geqslant 4$ (approximately) furnishes a reasonably good representation of the flow around a sphere rotating in an infinite medium for cases where $Re_1 \leqslant 45$. They also indicate that the results from this investigation approach those predicted from the Couette flow theory as $R_2/R_1 \to 1$ and are in good agreement with those obtained by Gagliardi[33] when $R_2/R_1 \leqslant 2{\cdot}5$ (approximately).

A comparison of the steady state torques (T_q) obtained by several investigators[5,7,24] is shown in Tables III(a) and III(b) for case studies a-IIA and a-IIB respectively. It can be seen from these tables that the results from this investigation are in fairly good agreement with those obtained by the other investigators.

Results for the impulsive torque problem

Typical results for contours of Ω and Ψ for the impulsive torque problem are shown in Figures 17 and 18 at $t = 0{\cdot}02$. Contours for additional cases can be found in Reference 34. As can be seen, the contours shown in these figures are in good agreement with those obtained by Gagliardi.[33] In general, the results obtained for the impulsive torque problem from this investigation were in good agreement with those obtained by Gagliardi[33] for all cases where $Re_2 \leqslant 100$.

Values of the viscous torques (T_q) are shown plotted as a function of time in Figures 19 and 20 for two cases. The figures show that the viscous torque on the outer sphere increases with time from zero to a maximum value and then decreases asymptotically back to zero. The corresponding plots of the angular velocity (ω_q) versus time for these cases are shown in Figures 21 and 22.

Table III. (a) Comparison of T_1 for case a-IIA. (b) Comparison of T_2 for case a-IIB

(a)	$-T_1$			
Re_2	Dennis and Singh[7]	Dennis and Quartapelle[24]	Munson and Joseph[5]	Present study
100	0·446	0·445	0·446	0·446
500	0·738	0·770	0·741	0·769
1000	0·978	1·039	0·986	1·010
2000	1·285	—	—	1·390

(b)	T_2			
Re_2	Dennis and Singh[7]	Dennis and Quartapelle[24]	Munson and Joseph[5]	Present study
100	0·500	0·517	0·501	0·499
500	0·715	0·781	0·720	0·716
1000	0·864	0·928	—	0·863
2000	1·069	—	—	1·068

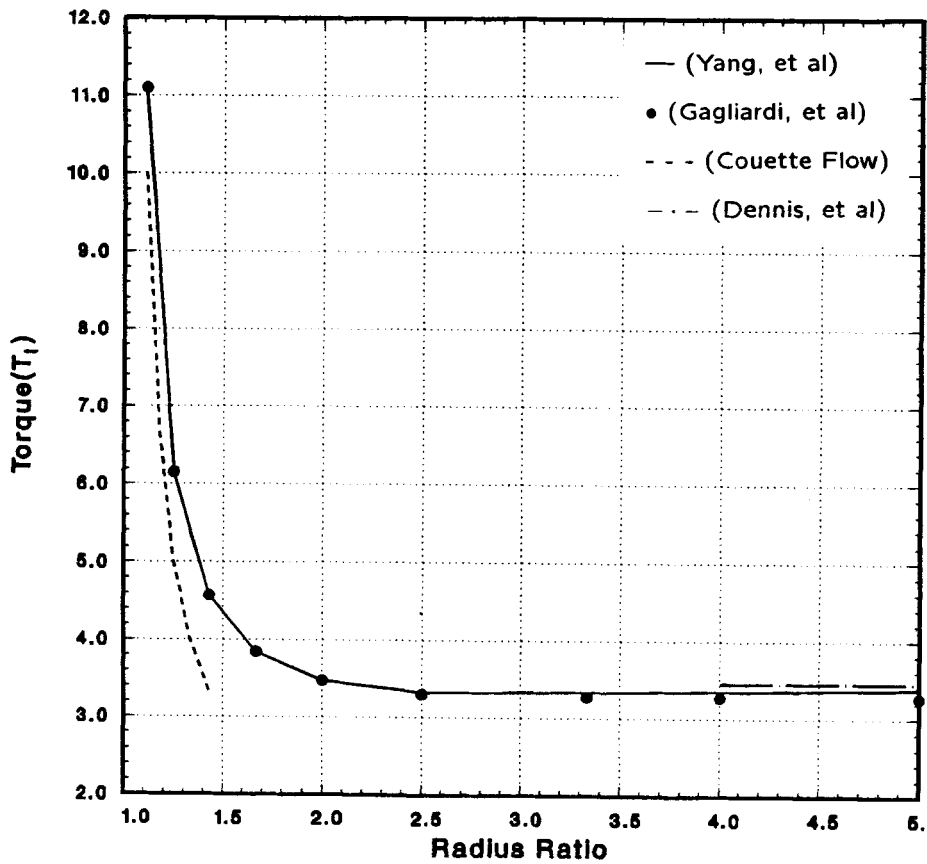

Figure 15. Plot of viscous torque (T_1) versus radius ratio; case study a-IIA ($Re_1 = 15$, steady state)

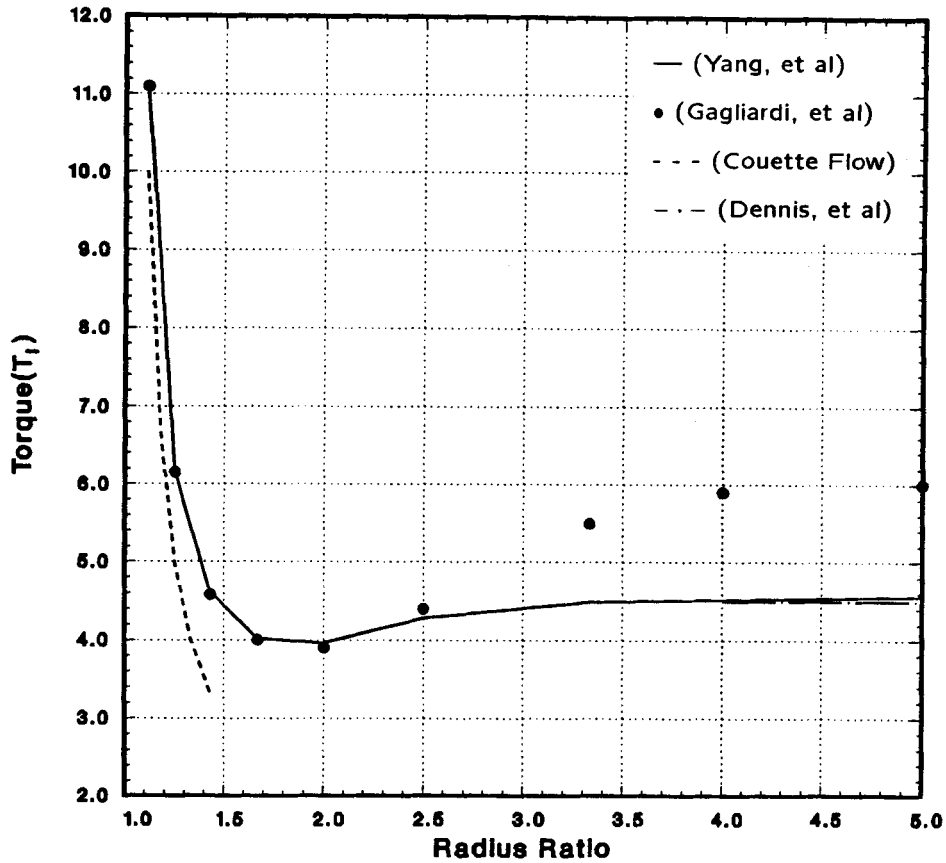

Figure 16. Plot of viscous torque (T_1) versus radius ratio; case study a-IIA ($Re_1 = 45$, steady state)

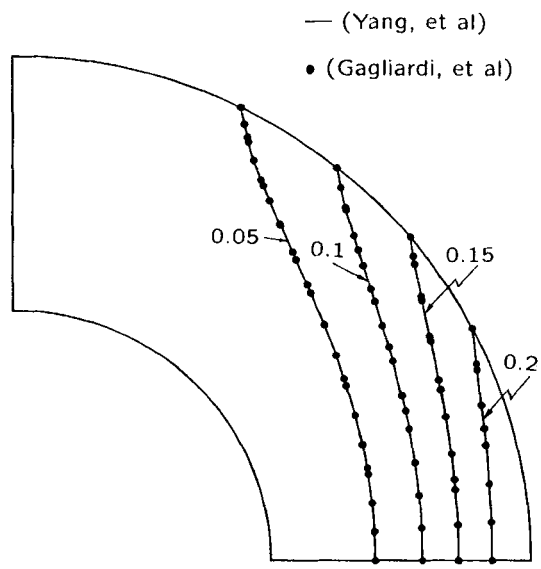

Figure 17. Plot of contour lines for Ω; case study b-IIB-1 ($t = 0{\cdot}02$)

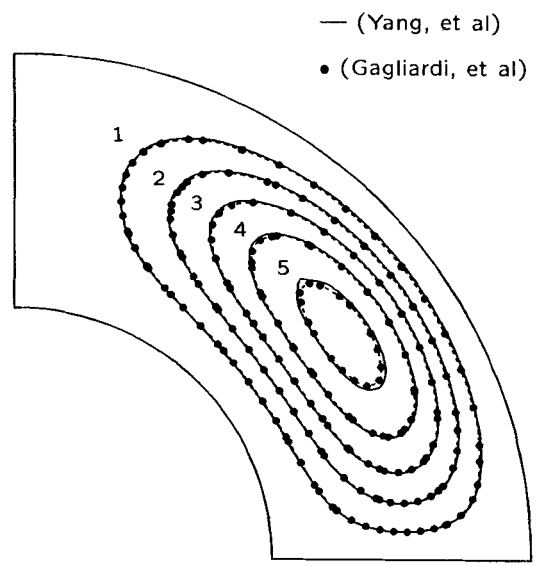

Figure 18. Plot of contour lines for $\Psi \times 10^4$; case study b-IIB-1 ($t = 0{\cdot}02$)

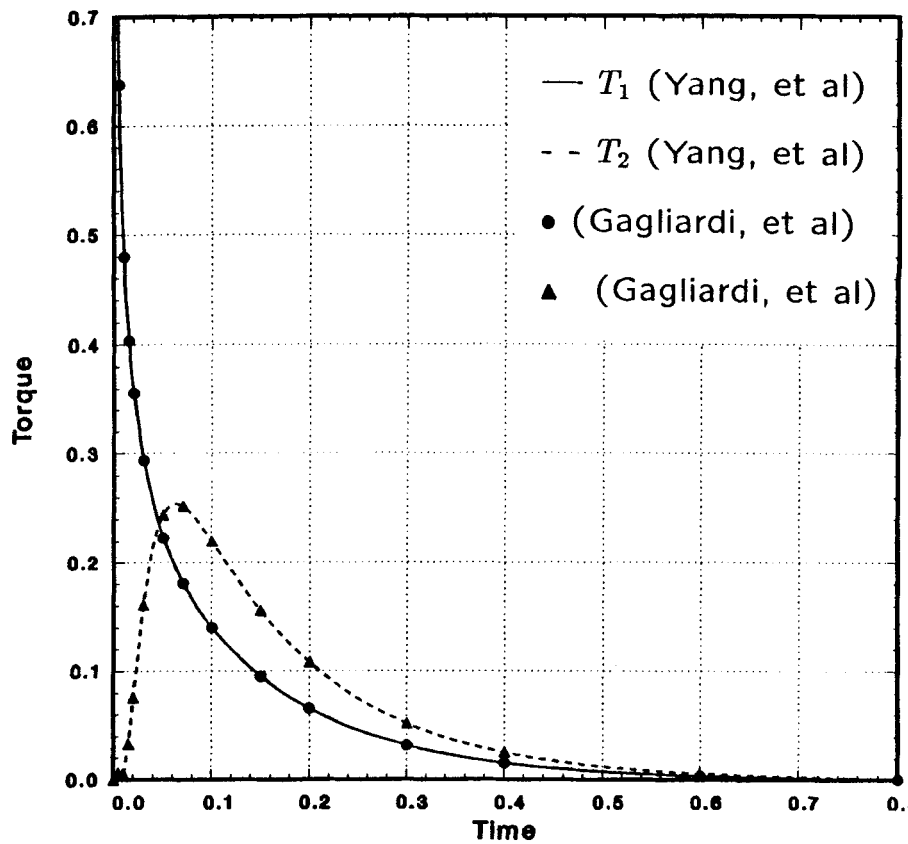

Figure 19. Plot of viscous torque versus time; case study b-IIA-1

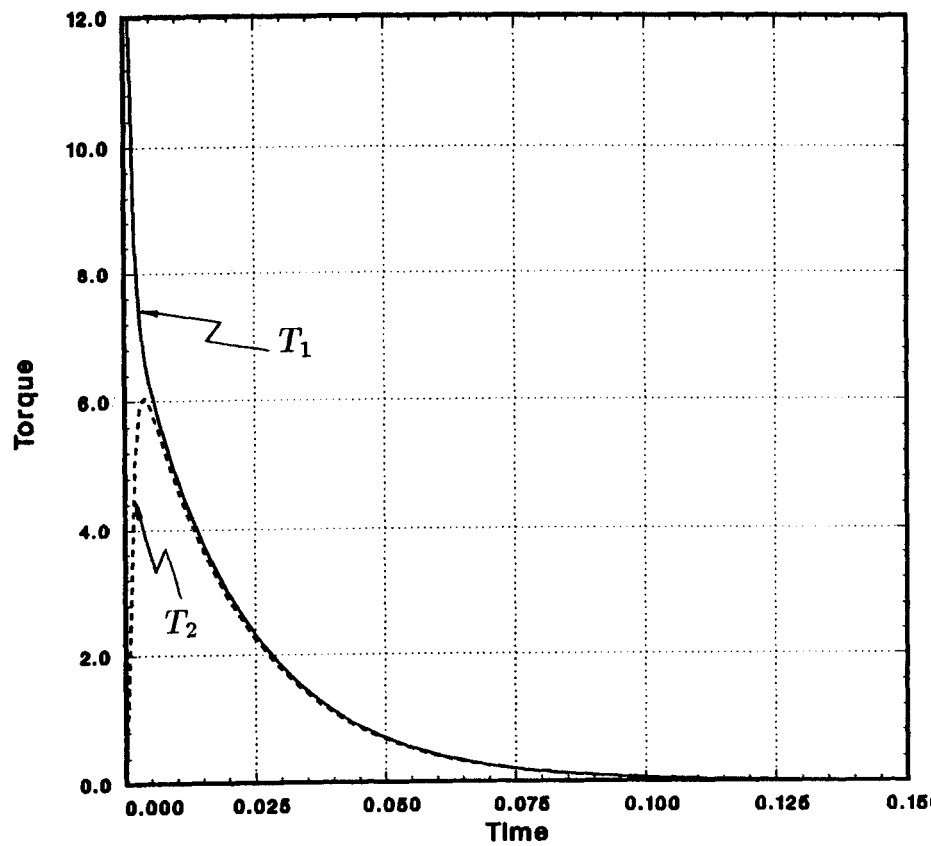

Figure 20. Plot of viscous torque versus time; case study b-IC-2

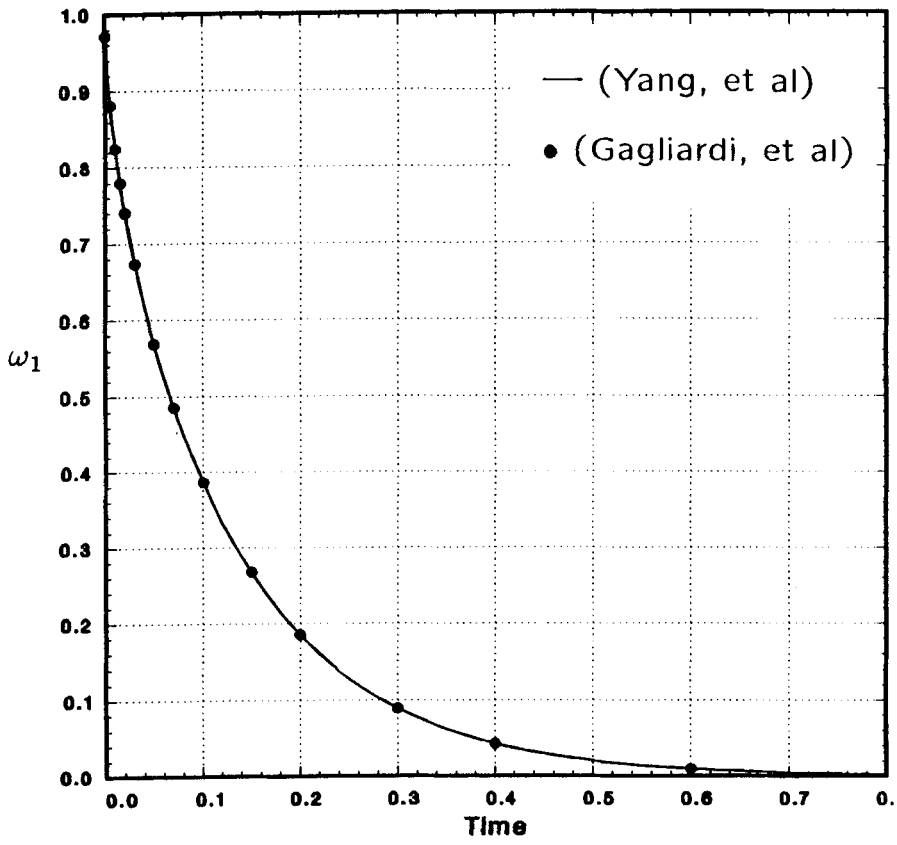

Figure 21. Plot of ω_1 versus time; case study b-IIA-1

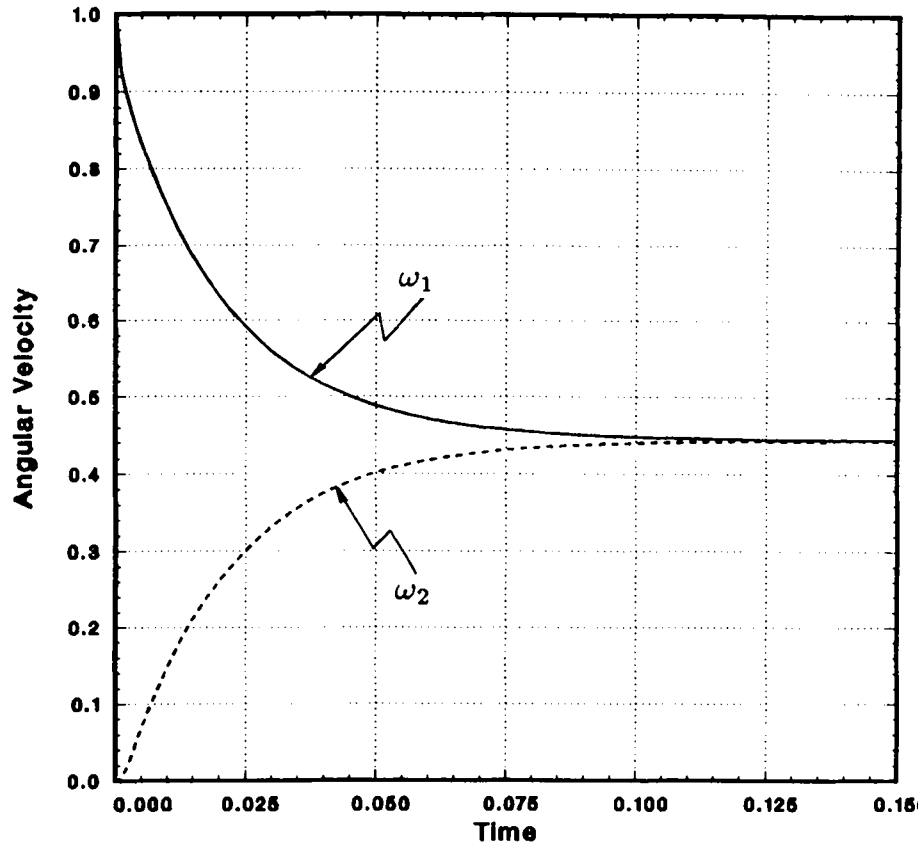

Figure 22. Plot of angular velocity versus time; case study b-IC-2

Figure 21 shows that the angular velocity of the inner sphere decays asymptotically from the initial value to zero, while Figure 22 shows that the angular velocities of the inner and outer spheres attain the same non-zero limiting value asymptotically. Figure 21 also shows that the results from this investigation are in good agreement with those obtained by Gagliardi.[33]

CONCLUSIONS

The primary purpose of this research was to study the use of a finite difference method to analyse the transient motion of a fluid contained in an annulus between two concentric spheres which are started suddenly by prescribed torques. With the approach adopted, only the derivatives with respect to spatial variables were approximated by the use of the finite difference derivative formulae. This led to a finite difference model comprised of a system of ordinary differential equations. This approach proved to be effective in view of the availability of efficient algorithms for solving these equations.

REFERENCES

1. I. Proudman, 'The almost-rigid rotation of viscous fluid between concentric spheres', *J. Fluid Mech.*, **1**, 505–516 (1956).

2. K. Stewartson, 'On almost rigid rotations Part 2', *J. Fluid Mech.*, **26,** 131–144 (1965).
3. G. F. Carrier, 'Some effects of stratification and geometry in rotating fluids', *J. Fluid Mech.*, **23,** 145–172 (1965).
4. W. C. Haberman, 'Secondary flow about a sphere rotating in a viscous liquid inside a coaxially rotating spherical container', *Phys. Fluids*, **5,** 625–626 (May 1962).
5. B. R. Munson and D. D. Joseph, 'Viscous incompressible flow between concentric rotating spheres. Part 1. Basic flow', *J. Fluid Mech.*, **49,** 289–303 (1971).
6. J. Pedlosky, 'Axially symmetric motion of a stratified rotating fluid in spherical annulus of a narrow gap', *J. Fluid Mech.*, **36,** 401–415 (1969).
7. S. C. R. Dennis and S. N. Singh, 'Calculation of the flow between two rotating spheres by the method of series truncation', *J. Comput. Phys.*, **28,** 297–314 (1978).
8. D. Greenspan, 'Numerical studies of steady, viscous, incompressible flow between two rotating spheres', *Comput. Fluids*, **3,** 68–82 (1975).
9. D. Schultz and D. Greenspan, 'Improved solution of steady, viscous, incompressible flow between two rotating spheres', *Comput. Fluids*, **7,** 157–163 (1979).
10. G. Schrauf, 'Branching of Navier–Stokes equations in a spherical gap', in E. Krause (ed.), *Eighth Int. Conf. on Numerical Methods in Fluid Dynamics; Lecture Notes in Physics, Vol. 170*, 1982, pp. 474–480.
11. P. Bar-Yoseph, J. J. Blech and A. Solan, 'Finite element solution of the Navier–Stokes equations in rotating flow', *Int. j. numer. methods eng.*, **17,** 1123–1146 (1981).
12. M. P. Sorokin, G. N. Khlebutin and G. F. Shaidurov, 'Study of the motion of a liquid between two rotating spherical surfaces', *J. Appl. Mech. Tech. Phys.*, **7** (6), 73–74 (1966).
13. G. N. Khlebutin, 'Stability of fluid motion between a rotating and a stationary concentric sphere', *Fluid Dyn.*, **3** (6), 31–32 (1968).
14. J. Zierep and O. Sawatzki, 'Three dimensional instabilities and vortices between two rotating spheres', *Eighth Symp. on Naval Hydrodynamics*, 1970, pp. 275–288.
15. B. R. Munson and M. Menguturk, 'Viscous incompressible flow between concentric rotating spheres. Part 3. Linear stability and experiments', *J. Fluid Mech.*, **69**, 705–719 (1975).
16. M. Wimmer, 'Experiments on a viscous flow between concentric rotating spheres', *J. Fluid Mech.*, **78,** 317–335 (1976).
17. M. Wimmer, 'Experiments on the stability of viscous flow between two concentric rotating spheres', *J. Fluid Mech.*, **103,** 117–131 (1981).
18. K. Nakabayashi, 'Frictional moment of flow between two concentric spheres, one of which rotates', *J. Fluid Eng.*, **100,** 97–106 (March 1978).
19. A. M. Waked and B. R. Munson, 'Torque characteristics for spherical annulus flow', *J. Fluid Eng.*, **101,** 284–286 (June 1979).
20. A. M. Waked and B. R. Munson, 'Laminar-turbulent flow in a spherical annulus', *J. Fluid Eng.*, **100,** 281–286 (September 1978).
21. B. R. Munson and R. W. Douglas, 'Viscous flow in oscillatory spherical annuli', *Phys. Fluids*, **22** (2), 205–208 (February 1979).
22. C. E. Pearson, 'A numerical study of the time dependent viscous flow between two rotating spheres', *J. Fluid Mech.*, **28,** 323–336 (1967).
23. C. E. Pearson, 'A numerical method for incompressible viscous flow problems in a spherical geometry', in *Studies in Numerical Analysis I*, SIAM, Philadelphia, PA, 1968, pp. 65–78.
24. S. C. R. Dennis and L. Quartapelle, 'Finite difference solution to the flow between two rotating spheres', *Comput. Fluids*, **12** (2), 79–92 (1984).
25. E. Krause and F. Bartels, 'Finite-difference solution of the Navier–Stokes equations for axially symmetric flows in spherical gaps', *Lecture Notes in Mathematics, Vol. 771*, 1979, pp. 313–322.
26. F. Bartels, 'Taylor vortices between two concentric rotating spheres', *J. Fluid Mech.*, **119,** 1–25 (1982).
27. C. R. Illingworth, 'Boundary layer growth on a spinning body', *Phil. Mag.*, **45** (Ser. 7), 1–8 (1954).
28. E. R. Benton, 'Laminar boundary layer on a impulsively started rotating sphere', *J. Fluid Mech.*, **23** (Part 3), 611–623 (1965).
29. K. E. Barrett, 'On the impulsively started rotating sphere', *J. Fluid Mech.*, **27** (Part 4), 779–788 (1967).
30. S. C. R. Dennis and D. B. Ingham, 'Laminar boundary layer on an impulsively started rotating sphere', *Phys. Fluids*, **22,** 1–9 (1979).
31. S. C. R. Dennis, S. N. Singh and D. B. Ingham, 'The steady flow due to a rotating sphere at low and moderate Reynolds numbers', *J. Fluid Mech.*, **101** (Part 2), 257–279 (1980).
32. H. Takagi, 'Viscous flow induced by slow rotation of a sphere', *J. Phys. Soc. Japan*, **42** (1), 319–325 (January 1977).
33. J. C. Gagliardi, 'Analytical studies of axially symmetric motion of an incompressible viscous fluid between two concentric rotating spheres', *Ph.D. Dissertation*, Marquette University, February 1987.
34. J.-K. Yang, 'Numerical studies of axially symmetric motion of an incompressible viscous fluid between two concentric rotating spheres', *Ph.D. Dissertation*, Marquette University, June 1987.